The American Journal of Pathology, Vol. 175, No. 4, October 2009

DOI: 10.2353/ajpath.2009.090035

Musculoskeletal Pathology

Role of MKP-1 in Osteoclasts and Bone Homeostasis

Jodi Carlson,* Weiguo Cui,† Qing Zhang,† Xiaoqing Xu,† Fatih Mercan,‡ Anton M. Bennett,‡ and Agnès Vignery†

From the Section of Comparative Medicine, Departments of Orthopaedics and Cell Biology,† and Department of Pharmacology,‡ Yale School of Medicine, New Haven, Connecticut*

Bone mass is maintained through the complementary activities of osteoblasts and osteoclasts; yet differentiation of either osteoblasts and osteoclasts engages the mitogen-activated protein kinase (MAPK) pathway. The MAPKs are negatively regulated by a family of dual-specificity phosphatases known as the MAPK phosphatases (MKPs). MKP-1 is a stress-responsive MKP that inactivates the MAPKs and plays a central role in macrophages; however, whether MKP-1 plays a role in the maintenance of bone mass has yet to be investigated. We show here, using a genetic approach, that *mkp-1*$^{-/-}$ female mice exhibited slightly reduced bone mass. We found that *mkp-1*$^{+/+}$ and *mkp-1*$^{-/-}$ mice had equivalent levels of bone loss after ovariectomy despite *mkp-1*$^{-/-}$ mice having fewer osteoclasts, suggesting that *mkp-1*$^{-/-}$ osteoclasts are hyperactive. Indeed, deletion of MKP1 led to a profound activation of osteoclasts *in vivo* in response to local lipopolysaccharide (LPS) injection. These results suggest a role for MKP-1 in osteoclasts, which originate from the fusion of macrophages. In support of these observations, receptor activator for nuclear factor-κB ligand induced the expression for MKP-1, and osteoclasts derived from *mkp-1*$^{-/-}$ mice had increased resorptive activity. Finally, receptor activator of nuclear factor-κB ligand-induced p38 MAPK and c-Jun NH_2-terminal kinase activities were enhanced in osteoclasts derived from *mkp-1*$^{-/-}$ mice. Taken together, these results show that MKP-1 plays a role in the maintenance of bone mass and does so by negatively regulating MAPK-dependent osteoclast signaling. ***(Am J Pathol 2009, 175:1564–1573; DOI: 10.2353/ajpath.2009.090035)***

Mitogen-activated protein kinases (MAPKs) constitute a family of serine/threonine protein kinases that transduce a wide array of extracellular signals into cellular responses, including cell growth, differentiation, and apoptosis. The three major subfamilies of MAPKs are extracellular signal-related kinases (ERKs), c-Jun NH_2-terminal kinase (JNK), and p38 MAPK.[1] MAPK activation occurs via phosphorylation on both threonine and tyrosine regulatory residues through the action of MAPK kinases, whereas dephosphorylation of either residue inactivates the MAPKs.[2,3] MAPKs have been implicated in the control of bone mass,[4] which is maintained by both osteoblasts and osteoclasts.

Osteoblasts are derived from mesenchymal stem cells and are responsible for the synthesis of the bone matrix and its subsequent calcification.[5,6] Although the physiological role of the MAPK pathway in osteoblasts had remained controversial,[7] recent work has established an important role for the ERK pathway in osteoblast differentiation that involves stimulation of RUNX2 phosphorylation and transcriptional activity.[7] Osteoclasts are multinucleate cells derived from the hematopoietic monocyte/macrophage lineage and are responsible for the degradation of mineralized bone. Receptor activator of nuclear factor-κB ligand (RANKL), which promotes differentiation and activation of osteoclasts, is expressed by osteoblasts, bone marrow stromal cells, and activated T-cells.[8–11] RANKL, on binding its receptor RANK, stimulates osteoclasts via the MAPK and the nuclear factor-κB pathways.[1,11] Whereas all three families of MAPKs become activated during osteoclastogenesis,[12–14] p38 MAPK plays a central role in RANKL-induced osteoclast differentiation.[12–14] Therefore, the activation of both osteoblasts and osteoclasts requires engagement of the MAPK pathway to maintain bone mass.

The primary phosphatases responsible for regulating MAPK signaling are the MAPK phosphatases (MKPs), which constitute a subfamily of dual-specificity

Supported by the National Institutes of Health (grants AR46504 to A.M.B. and DE12110 to A.V.).

A.M.B. and A.V. contributed equally to this work.

Accepted for publication July 7, 2009.

Address reprint requests to Agnès Vignery, D.D.S, Ph.D., Department of Orthopaedics and Rehabilitation, Yale University School of Medicine, 333 Cedar St., New Haven, CT 06510. E-mail: agnes.vignery@yale.edu.

phosphatases. The family of MKPs includes 11 members that have distinct and overlapping affinities for the MAPKs. The ability of the MKPs to selectively dephosphorylate the MAPKs is dictated by the kinase interaction motif, which resides in the noncatalytic region of the MKPs.[15,16] Direct binding between the MKPs and the MAPKs, in most cases, stimulates MKP-mediated dephosphorylation of the MAPKs. The founding member of the MKP family, MKP-1, is an inducible nuclear MKP that inactivates all three groups of MAPKs, with a preference for p38 MAPK and JNK over ERK.[15,16] Because MKP-1 has been shown to be an important negative regulator of the MAPK pathway in the innate immune response,[17–21] hence macrophages, and because MAPKs are essential for both osteoblast and osteoclast activities,[2] we hypothesized that MKP-1 might play a role in the control of bone mass. Here we show that MKP-1-deficient (*mkp-1*$^{-/-}$) female mice exhibited transiently reduced bone mass, suggesting that MKP-1 plays a role in bone homeostasis. We found that *mkp-1*$^{+/+}$ and *mkp-1*$^{-/-}$ mice had equivalent levels of bone loss after ovariectomy despite *mkp-1*$^{-/-}$ mice having fewer osteoclasts. Osteoclasts derived from *mkp-1*$^{-/-}$ mice exhibited enhanced resorption and p38 MAPK and JNK activation. Taken together, MKP-1 plays a role in the maintenance of bone mass and does so by negatively regulating MAPK-dependent osteoclast signaling.

Materials and Methods

Animals

mkp-1$^{-/-}$ mice were generated on a mixed 129J/C57BL6 background, bred, and genotyped as described previously.[22,23] The animals were housed in standard caging on a 12-hour light cycle and were offered free access to rodent chow (number 2018, Harlan Teklad, Madison, WI) and water. Baseline mice were euthanized at 8 weeks of age. Female *mkp-1*$^{+/+}$ and *mkp-1*$^{-/-}$ mice were subjected to ovariectomy at 8 weeks of age and were euthanized 6 weeks later, along with age-matched controls. Mice received two i.p. injections of calcein (5 mg/kg/day) on days 8 and 1 before sacrifice for dynamic histomorphometric analysis. To assess osteoclast formation and activity *in vivo*, we administered a single local s.c. calvarial injection of lipopolysaccharide (25 μg in 2 μl; *Escherichia coli* O55:B5, Sigma Chemical, St. Louis, MO) to 8-week-old male and female mice that were sacrificed 5 days later. Calvariae were subjected to micro-computed tomography (CT) analysis, and resorbed areas were quantified using ImageJ software (NIH, Bethesda, MD). All procedures were approved by the Yale University Institutional Animal Care and Use Committee.

Reagents

Rabbit polyclonal antibodies directed against p38 MAPK, phosphorylated (p) p38 (p-p38 MAPK), ERK1/2, p-ERK1/2, JNK, and p-JNK, and a mouse monoclonal antibody directed against inhibitor of nuclear factor-κB were obtained from Cell Signaling Technology (Beverly, MA). Anti-MKP-1 antibodies were obtained from Santa Cruz Biotechnology (Santa Cruz, CA). A mouse monoclonal antibody directed against Grp94 was purchased from Abcam (Cambridge, MA). Horseradish peroxidase-conjugated F(ab′)$_2$ directed against rabbit and mouse IgG were purchased from Jackson ImmunoResearch (West Grove, PA). Phalloidin-Alexa Fluor 568 was purchased from Invitrogen (Carlsbad, CA), and Osteologic slides were from BD Biosciences (Franklin Lakes, NJ). Rat anti-mouse monoclonal antibodies used for flow cytometry included anti-Mac-1 (CD11b) conjugated to fluorescein (Mac1-FITC; M1/70) and rat FITC-IgG2b (PharMingen, San Diego, CA); anti-c-fms conjugated to phycoerythrin (c-fms-PE; IgG2b), and anti-c-Kit conjugated to allophycocyanin (c-kit-APC; IgG2b) and isotype-matching antibodies (eBioscience, San Diego, CA). Secondary antibody anti-rat IgG2a conjugated to FITC was purchased from PharMingen. Phalloidin-Alexa Fluor 568 was purchased from Invitrogen. All supplies and reagents for tissue culture were endotoxin-free. Some bone marrow cells were treated with polymyxin B sulfate for 24 hours to avoid the effects of the endotoxin before treatment. All supplies and reagents for tissue culture were endotoxin-free. Unless otherwise stated, all chemicals were from Sigma Chemical.

Osteoclast Formation and Activity

Bone marrow- and spleen-derived osteoclasts were generated from 4- to 12-week-old *mkp-1*$^{+/+}$ and *mkp-1*$^{-/-}$ mice as described previously.[24] Bone marrow and spleen cells were isolated, mechanically dissociated, and cultured at a density of 1.33×10^6 cells per cm^2 in minimal essential medium containing 10% heat-inactivated fetal bovine serum (HyClone, Logan, UT), 100 units/ml penicillin-streptomycin (Gibco Invitrogen, Carlsbad, CA), 1% minimal essential medium vitamins, 1% glutamine, and 30 ng/ml macrophage colony-stimulation factor (M-CSF) (PeproTech, Inc, Rocky Hill, NJ). Medium was changed every 3 days. The RANKL dose response was determined by culturing cells in 20 to 100 ng/ml RANKL in increments of 20 ng/ml. After 6 days of culture, the cells were fixed and reacted for tartrate-resistant acid phosphatase according to the supplier's directions. To assess the formation of an actin ring, a landmark of osteoclast activity, cells were cultured in the presence of M-CSF (20 ng/ml) and RANKL (PreproTech, Inc., 100 ng/ml) on glass slides for 8 days, fixed, and reacted with phalloidin-Alexa Fluor 568 and Topro-3. To further assess resorptive activity, cells were cultured on Osteologic slides that were coated with artificial bone made of calcium phosphate crystals. After 20 days, cells were lysed, and the calcium phosphate substrate was stained with silver nitrate according to the supplier's instructions. The resorbed areas on slides were recorded by histomorphometry. Osteoblast alkaline phosphatase and mineral-

ized nodule formation assays were performed as we described previously[25] using 4- to 12-week-old *mkp-1*$^{+/+}$ and *mkp-1*$^{-/-}$ mice.

Western Blot Analysis

After 7 days of culture, osteoclasts were serum-starved for 2 hours and stimulated with the indicated reagents. The cells were then lysed in Laemmli sample buffer supplemented with protease inhibitors (Complete Tablets, Roche Molecular Biochemicals, Indianapolis, IN), sodium fluoride, and a phosphatase inhibitor cocktail II. The lysates were sonicated and resolved by SDS-polyacrylamide gel electrophoresis, transferred to Immobilon-P membranes, and subjected to immunoblotting using enhanced chemiluminescence (Amersham Pharmacia Biotechnology, Sunnyvale, CA). Blots were quantified using ImageJ software. Numbers represent the average of three experiments, with values equilibrated against their corresponding controls.

Flow Cytometry

Cells were stained with the first antibody, incubated for 30 minutes on ice, and washed twice with washing buffer (5% fetal calf serum/PBS). The secondary antibody was added, and the cells were incubated for 30 minutes on ice. After incubation, cells were washed twice with washing buffer and suspended in washing buffer for fluorescence-activated cell sorter analysis, which was performed using a FACSCalibur (BD Biosciences).

Bone Density and Microarchitecture

Bone density was determined as described previously[26] by peripheral quantitative computed tomography (pQCT) (XCT Research M, Norland Medical Systems, Fort Atkinson, WI) of a virtual 1-mm cross section of the distal femur 0.25 mm proximal to the growth plate. In addition, distal femurs and calvariae were scanned with a micro-CT scanner (MicroCT 40, Scanco, Bassersdorf, Switzerland) with a 2048 $\times$ 2048 matrix and isotropic resolution of 9 μm^3 with 12 μm voxel size.

Histomorphometry

Femurs from *mkp-1*$^{+/+}$ and *mkp-1*$^{-/-}$ mice were dehydrated in a graded ethanol series and embedded without decalcification in methylmethacrylate, as described previously.[26] Four-micrometer-thick cross sections of the distal femur 0.25 mm proximal to the growth plate were stained with Villanueva mineralized bone stain for static histomorphometric analysis, and 8-μm-thick sections were left unstained for analysis of dynamic parameters. Histomorphometric analysis was performed using Osteomeasure software (Osteometrics, Atlanta, GA). The following parameters were measured: the relative tissue surface occupied by bone (%); the number of trabeculae per mm; the relative surface of bone occupied by trabeculae (%); the distance/separation between trabeculae (μm); the number of osteoclasts per total bone surface; the perimeter of osteoclasts per total bone perimeter; the perimeter of osteoblasts per total bone perimeter; mineralizing surface; mineral apposition rate; and bone formation rate.

Statistical Analysis

Data represent the mean $\pm$ 1 SD. Treatment groups were compared using analysis of variance. Pairwise comparison *P* values between the treatment groups were adjusted using Tukey's multiple comparison procedure. Statistical significance was declared if two-sided *P* value was <0.05. All computations were performed using SPSS.

Results

Lack of MKP-1 Is Associated with a Reduced Trabecular Bone Density in Female Mice

To assess the role of MKP-1 in the maintenance of bone mass, we subjected femurs from 8-week-old *mkp-1*$^{+/+}$ and *mkp-1*$^{-/-}$ male and female mice to micro-CT analysis. The femurs revealed little distinguishable differences between male *mkp-1*$^{+/+}$ compared with *mkp-1*$^{-/-}$ mice (data not shown) and between female *mkp-1*$^{+/+}$ compared with *mkp-1*$^{-/-}$ mice (Figure 1A). Similar results were also obtained by X-ray analysis (data not shown). Next, we subjected the distal femurs from 8-week-old *mkp-1*$^{+/+}$ and *mkp-1*$^{-/-}$ male and female mice to pQCT analysis. Female but not male *mkp-1*$^{-/-}$ mice (data not shown) showed a 19% reduction in trabecular density and a 15% reduction in trabecular content (Figure 1B). This observation was confirmed by histomorphometric analysis, which revealed a decrease in the number and surface area of trabeculae that was associated with a concomitant increase in the separation between the trabeculae of *mkp-1*$^{-/-}$ female compared with *mkp-1*$^{+/+}$ female mice (Figures 1, C and D; Table 1). We also observed a trend toward reduced osteoclast number in *mkp-1*$^{-/-}$ mice compared with *mkp-1*$^{+/+}$ mice (Figure 1E). In contrast, dynamic histomorphometric analysis of long bones revealed that the bone formation rate was similar in wild-type and MKP-1-deficient mice (Table 1), suggesting that osteoblasts are not affected by the absence of MKP-1. Although MAPKs have been shown to positively regulate osteoblast and osteoclast activities, our results suggest that the effect of MKP-1 probably occurs in osteoclasts rather than in osteoblasts.

Reduced Osteoclast Number but Equivalent Bone Loss after Estrogen-Depletion of mkp-1$^{-/-}$ Mice

Estrogen has been shown to reduce osteoclast formation and activation directly via suppression of RANK-

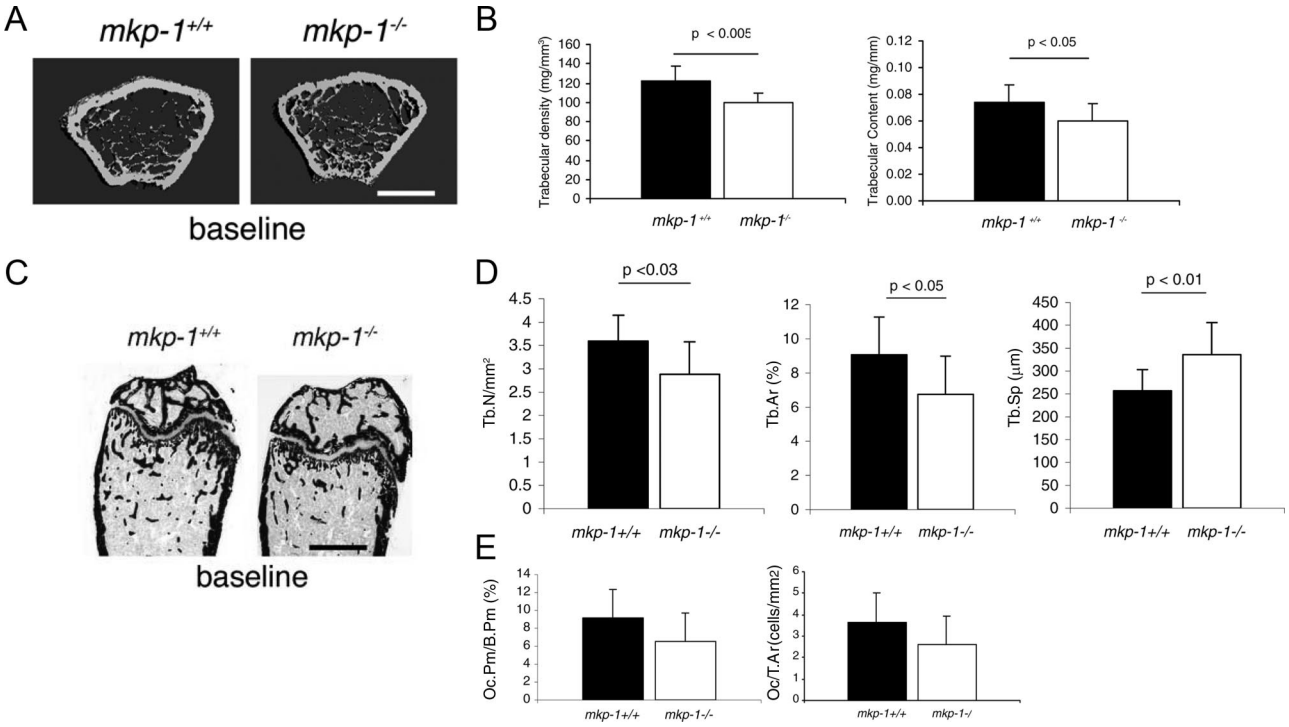

Figure 1. Female *mkp-1*$^{-/-}$ mice have less trabecular bone than *mkp-1*$^{+/+}$ mice. Eight-week-old female *mkp-1*$^{-/-}$ and *mkp-1*$^{+/+}$ mice were used as a baseline. Representative distal femurs were scanned using micro-CT (**A**) and pQCT (**B**). Scale bar = 1 mm. **C:** Femurs were embedded in methylmethacrylate, sectioned, stained with Villanueva mineralized bone stain, and subjected to bone histomorphometric analysis. Scale bar = 1 μm. **D:** Number of trabeculae per μm^2, relative surface of bone occupied by trabeculae (%), and distance/separation between trabeculae (μm). **E:** Relative osteoclast perimeter versus bone perimeter and osteoclast number per unit of bone surface (cells/mm^2). Data are means ± SD; $n = 8$.

induced signaling in osteoclast precursors.[15,16] Estrogen depletion induced by ovariectomy is a well established animal model for postmenopausal osteoporosis. Because MKP-1 is a stress-responsive immediate-early gene, we determined whether bone loss induced by estrogen depletion would be aggravated in the absence of MKP-1. We subjected 8-week-old *mkp-1*$^{+/+}$ and *mkp-1*$^{-/-}$ female mice to bilateral ovariectomy and sacrificed them 6 weeks later, at a time when bone remodeling has reached a new level of equilibrium, using age-matched mice as controls. We then analyzed distal femurs by micro-CT, pQCT, and histomorphometry. Micro-CT analysis suggested that ovariectomy induced comparable losses in trabecular

Table 1. Histomorphometric Analysis of Femurs from 8-week-old *mkp-1*$^{+/+}$ and *mkp-1*$^{-/-}$ Male and Female Mice

	Baseline			
	Male *mkp-1*$^{+/+}$	Male *mkp-1*$^{-/-}$	Female *mkp-1*$^{+/+}$	Female *mkp-1*$^{-/-}$
Static parameters				
Relative tissue surface occupied by bone (%)	12.64 ± 4.03	13.63 ± 3.80	9.07 ± 2.21	6.75 ± 2.23
Tb.Wi (μm)	30.54 ± 4.31	29.70 ± 3.72	27.54 ± 4.01	25.50 ± 2.58
No. of trabeculae (/mm)	4.57 ± 1.16	5.04 ± 0.99	3.60 ± 0.55	2.88 ± 0.70
Distance/separation between trabeculae (μm)	204.92 ± 79.37	176.28 ± 46.28	256.60 ± 46.94	335.60 ± 70.24*
Perimeter of osteoblasts per total bone perimeter (%)	9.06 ± 7.69	6.74 ± 2.55	13.11 ± 3.07	11.96 ± 4.74
Perimeter of osteoclasts per total bone perimeter (%)	4.62 ± 1.81	6.65 ± 2.06	9.16 ± 3.20	6.53 ± 1.85
No. of osteoclasts per total bone surface (cells/mm^2)	1.87 ± 0.70	2.71 ± 0.84	3.64 ± 1.36	2.59 ± 0.69
Dynamic parameters				
Mineral apposition rate (μm/day)	1.88 ± 0.56	1.95 ± 0.60	1.53 ± 0.41	1.56 ± 0.59
Bone formation rate/bone volume (mm^3/mm^3/year)	607.63 ± 381.22	530.36 ± 433.59	757.40 ± 366.73	492.38 ± 211.50
Bone formation rate/bone surface (mm^3/mm^2/year)	25.91 ± 11.15	27.05 ± 20.18	33.12 ± 18.14	20.40 ± 80.66

Values are mean ± SD.
*$P < 0.05$ versus baseline female *mkp-1*$^{+/+}$.

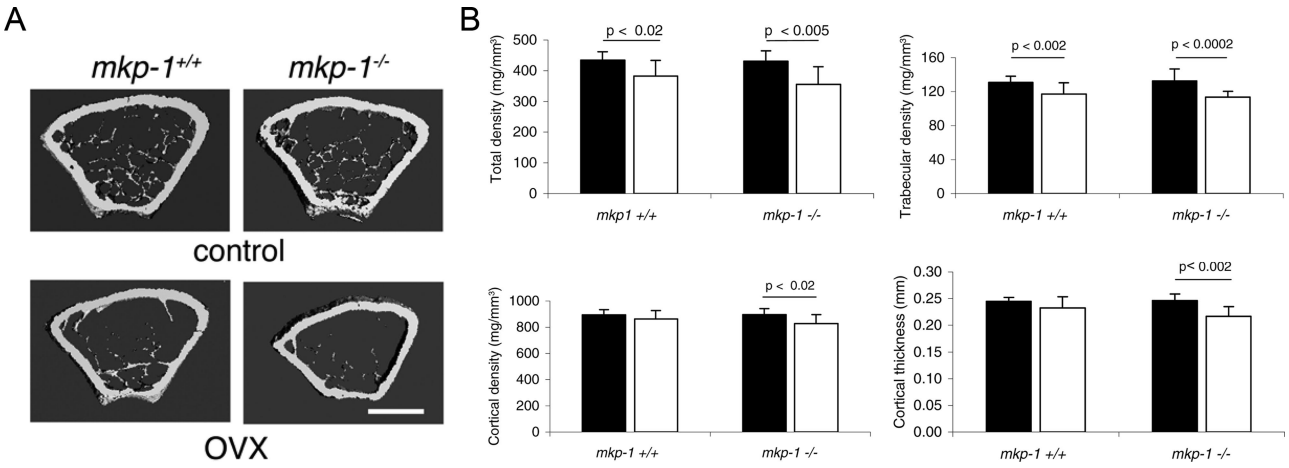

Figure 2. *mkp-1*$^{-/-}$ and *mkp-1*$^{+/+}$ mice lose equivalent amounts of bone in response to estrogen depletion. Eight-week-old *mkp-1*$^{-/-}$ and *mkp-1*$^{+/+}$ mice were subjected to ovariectomy (OVX), sacrificed 6 weeks later, and compared with age-matched controls. Femurs were analyzed by micro-CT (**A**) and pQCT (**B**). Total density, trabecular bone density, cortical bone density, and cortical thickness are shown: black bar, control; white bar, OVX. Data are means ± SD; $n = 8$.

bone density in *mkp-1*$^{+/+}$ and *mkp-1*$^{-/-}$ mice (Figure 2A). pQCT analysis confirmed that observation and revealed that *mkp-1*$^{-/-}$ mice exhibited a decrease in cortical bone density and a decrease in cortical thickness, whereas *mkp-1*$^{+/+}$ mice remained unaffected (Figure 2B). However, no significant difference was observed in either cortical bone density or cortical thickness in *mkp-1*$^{-/-}$ mice compared with *mkp-1*$^{+/+}$ mice after ovariectomy (Figure 2B). Of note, knockout female mice, which were 6 weeks older than baseline mice, no longer showed a difference from wild-type female mice, suggesting the transient nature of the bone phenotype, which dissipates with aging.

On histomorphometric analysis of the distal femurs, both *mkp-1*$^{+/+}$ and *mkp-1*$^{-/-}$ mice had fewer and smaller trabeculae associated with an increase in the separation between trabeculae as a result of ovariectomy. However, there were no differences between *mkp-1*$^{+/+}$ and *mkp-1*$^{-/-}$ mice (Figure 3, A and B; Table 2). Notably, despite equivalent loss of trabecular and cortical bone induced by estrogen depletion in *mkp-1*$^{-/-}$ mice compared with *mkp-1*$^{+/+}$ mice (Figures 2 and 3A), we found that trabecular bone from *mkp-1*$^{-/-}$ mice contained fewer osteoclasts that covered less bone surface compared with *mkp-1*$^{+/+}$ mice (Figure 3C). Dynamic histomorphometric analysis of long bones revealed that the bone formation rate was similar in wild-type and MKP-1-deficient mice (Table 2), suggesting that osteoblasts are not affected by the absence of MKP-1. Taken together, these data suggest that the absence of MKP-1 does not aggravate bone loss in response to estrogen depletion. However, remarkably, despite the fact that the extent of bone loss was comparable between *mkp-1*$^{+/+}$ and *mkp-1*$^{-/-}$ mice, after estrogen depletion *mkp-1*$^{-/-}$ mice achieved this with fewer osteoclasts. This observation raises the possibility that osteoclasts from MKP-1-deficient mice may be hyperactive or osteoblasts may be hypoactive or

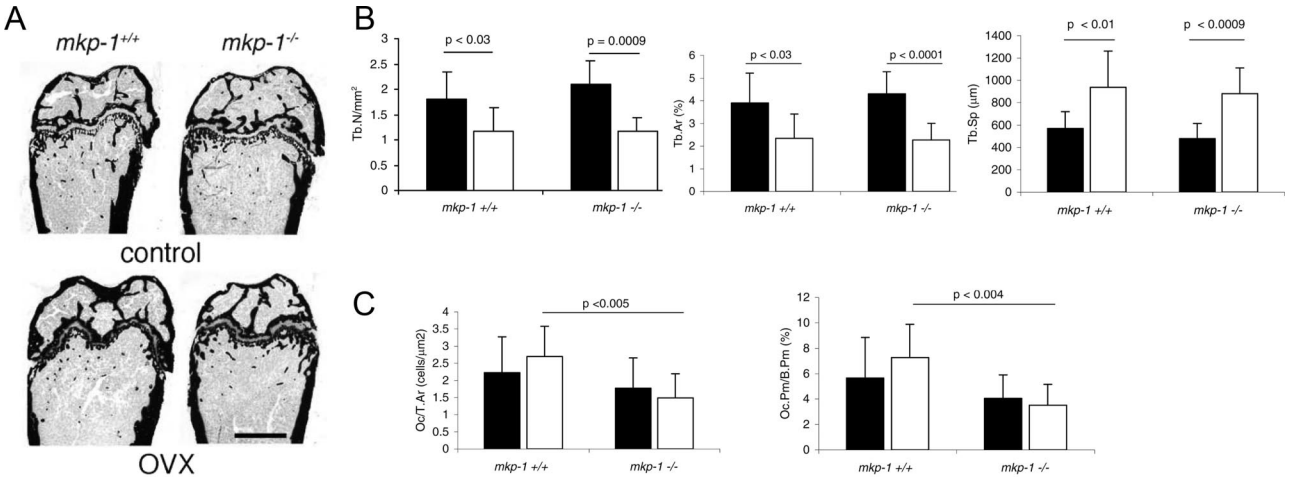

Figure 3. *mkp-1*$^{-/-}$ mice have fewer osteoclasts than *mkp-1*$^{+/+}$ mice in response to estrogen depletion. **A**, **B** and **C**: Eight-week-old *mkp-1*$^{-/-}$ and *mkp-1*$^{+/+}$ mice were subjected to ovariectomy (OVX), sacrificed 6 weeks later, and compared with age-matched controls. Femurs were analyzed by histomorphometry: Tb.N/μm^2, number of trabeculae per μm^2; Tb.Ar (%), relative surface of bone occupied by trabeculae; Tb.Sp (μm), distance/separation between trabeculae. Oc/T.Ar, number of osteoclasts per total bone surface; Oc.Pm./B.Pm (%), relative perimeter occupied by osteoclasts per total bone perimeter. Data are means ± SD; $n = 8$.

Table 2. Histomorphometric Analysis of Distal Femurs from 14-week-old Ovariectomized and Age-Matched Control *mkp-1*$^{+/+}$ and *mkp-1*$^{-/-}$ Female Mice

	Control		Ovariectomized	
	mkp-1$^{+/+}$	*mkp-1*$^{-/-}$	*mkp-1*$^{+/+}$	*mkp-1*$^{-/-}$
Static parameters				
Relative tissue surface occupied by bone (%)	3.90 ± 1.32	4.31 ± 0.96	2.35 ± 1.07*	2.27 ± 0.73†
Trabecular bone width (μm)	23.83 ± 2.23	22.72 ± 1.71	21.76 ± 2.61	21.07 ± 2.50
No. of trabeculae (/mm)	1.80 ± 0.55	2.10 ± 0.46	1.18 ± 0.47*	1.17 ± 0.28†
Distance/separation between trabeculae (μm)	569.56 ± 152.42	479.41 ± 135.22	937.45 ± 326.00*	881.96 ± 230.07†
Perimeter of osteoblasts per total bone perimeter (%)	12.62 ± 5.25	13.01 ± 6.28	8.57 ± 5.71	12.64 ± 3.82
Perimeter of osteoclasts per total bone perimeter (%)	5.65 ± 2.60	4.05 ± 1.66	7.27 ± 3.24	3.51 ± 1.45‡
No. of osteoclasts per total bone surface (cells/mm^2)	2.23 ± 1.04	1.78 ± 0.88	2.70 ± 0.88	1.49 ± 0.70‡
Dynamic parameters				
Mineral apposition rate (μm/day)	1.02 ± 0.61	1.19 ± 0.63	1.57 ± 0.47	1.36 ± 0.76
Bone formation rate/bone volume (mm^3/mm^3/year)	457.00 ± 230.87	494.53 ± 344.08	374.67 ± 148.15	595.99 ± 229.92
Bone formation rate/bone surface (mm^3/mm^2/year)	20.08 ± 10.07	19.03 ± 14.32	13.51 ± 13.51	20.10 ± 8.52

Values are mean ± SD.
*$P < 0.05$ versus control *mkp-1*$^{+/+}$.
†$P < 0.001$ versus control *mkp-1*$^{-/-}$.
‡$P < 0.005$ versus ovariectomized *mkp-1*$^{+/+}$.

both. MKP-1-deficient mice could conceivably contribute to an equivalent level of bone loss compared with wild-type mice using fewer osteoclasts.

MKP-1 Negatively Regulates Osteoclast Differentiation and Activation in Response to Local Lipopolysaccharide Injection

To determine whether MKP1 modulates osteoclast formation and activity *in vivo*, we used an efficient and rapid *in vivo* bone resorption assay. We injected mice with LPS in the periosteum of the right calvaria, which we subjected 5 days later to micro-CT analysis. As shown in Figure 4, mice deficient in MKP1 demonstrated extensive bone resorption, which was relatively discrete in wild-type mice. Indeed, resorption of bone extended beyond the injected site in MKP1-deficient mice, suggesting that MKP1 down-regulates osteoclast formation and activation. Whether this resorption was completed by fewer osteoclasts remains an open question.

MKP-1 Negatively Regulates Osteoclast Activity

To examine first whether MKP-1 affects the number of osteoclast precursors, we subjected freshly isolated bone marrow cells to flow cytometric analysis using surface markers expressed by pre-osteoclasts.[25] The percentage of precursor cells relative to the total number of bone marrow cells was similar in *mkp-1*$^{+/+}$ and *mkp-1*$^{-/-}$ mice (Figure 5A). To next determine whether deletion of MKP-1 results in the hyperactivation of osteoclasts, we cultured equal numbers of macrophages derived from spleen cells isolated from *mkp-1*$^{-/-}$ and age-matched *mkp-1*$^{+/+}$ mice in the presence of M-CSF (20 ng/ml) and increasing concentrations of RANKL. As expected, RANKL induced the differentiation of osteoclasts in a dose-dependent manner as seen by multinucleation and positive staining for the osteoclast marker tartrate-resistant acid phosphatase (Figure 4A). Although macrophages that lack MKP-1 formed osteoclasts, they were reduced in number compared with *mkp-1*$^{+/+}$ osteoclasts (Figure 5, A and B). We also found that *mkp-1*$^{-/-}$ osteoclasts occupied a reduced surface area (Figure 5C) and were significantly smaller than wild-type osteoclasts.

To actively resorb bone, osteoclasts form an actin "ring," which is a complex molecular attachment structure that seals off an extracellular compartment located between the cell and its substrate.[27] By virtue of being sealed off, this compartment can reach a low pH, which allows for the dissolution of hydroxyapatite crystals, and is rich in lysosomal enzymes that degrade the bone matrix under low pH conditions.[27] Therefore, the ring is the functional signature of active osteoclasts and because of its rich actin content, it can be visualized using phalloidin conjugated with a fluorescent marker. To determine whether MKP-1 plays a role in osteoclast activity, we cultured spleen-derived macrophages from *mkp-1*$^{+/+}$ and *mkp-1*$^{-/-}$ mice on glass slides for 8 days in the presence of M-CSF (30 ng/ml) and RANKL (50 ng/ml) and assessed ring formation. Whereas both *mkp-1*$^{+/+}$ and *mkp-1*$^{-/-}$ osteoclasts formed actin rings in response to RANKL, osteoclasts as well as their rings were notably smaller in *mkp-1*$^{-/-}$ osteoclasts compared with those in *mkp-1*$^{+/+}$ osteoclasts (Figure 6A). To determine whether the actin ring from cells that lack MKP-1 seals off a low pH compartment, we cultured equal numbers of spleen cell-derived macrophages from *mkp-1*$^{+/+}$ and *mkp-1*$^{-/-}$ mice on calcium phosphate-coated chamber slides in the

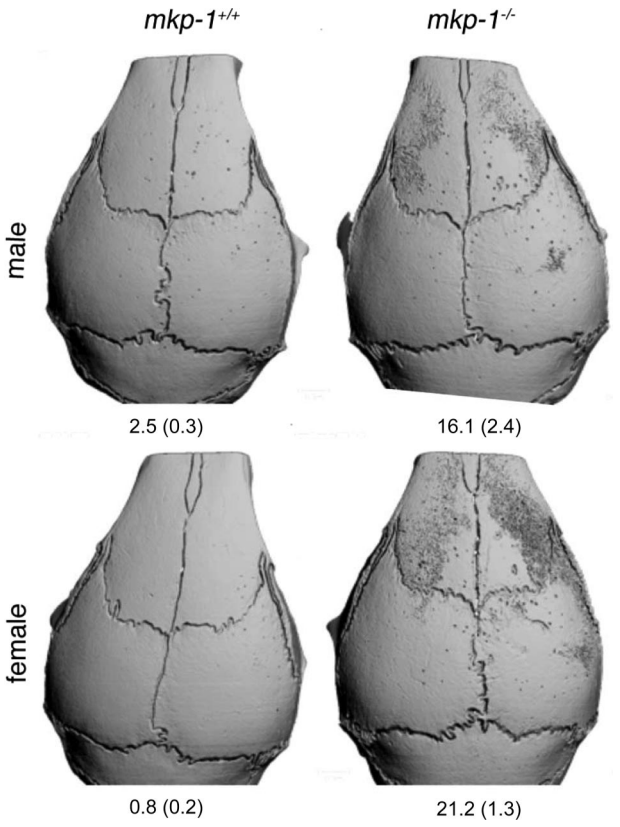

Figure 4. Absence of MKP-1 dramatically accentuates bone resorption in response to local injection of LPS. Eight-week-old *mkp-1*$^{-/-}$ and *mkp-1*$^{+/+}$ male and female mice were injected with 25 μg of LPS in a 2-μl volume in the periosteum of the right calvaria. Note the dramatic response of MKP1-deficient mice to LPS. Numbers represent mean % (±SD) resorbed bone surface. $n = 4$.

presence of M-CSF (20 ng/ml) and RANKL (50 ng/ml). Despite their smaller size and number, *mkp-1*$^{-/-}$ osteoclasts resorbed more calcium phosphate substrate per unit of surface area than *mkp-1*$^{+/+}$ osteoclasts (Figure 6, B and C). Collectively, these results demonstrate that MKP-1-deficient osteoclasts are hyperactive, indicating that MKP-1 negatively regulates osteoclast activity.

MKP-1 Is Essential for RANKL-Induced MAPK Inactivation in Osteoclasts

The MAPK pathway has been shown previously to play a critical role in stimulating osteoclast formation and activity.[12–14] Therefore, to provide a mechanism for the suppressive effect of MKP-1 on osteoclast activity, we determined whether MKP-1 participates in the inactivation of the MAPKs in osteoclasts. We cultured bone marrow-derived macrophages from *mkp-1*$^{+/+}$ and *mkp-1*$^{-/-}$ mice in the presence of M-CSF (30 ng/ml) and RANKL (50 ng/ml) for 7 days. After a 2-hour starvation, osteoclasts were stimulated with RANKL (100 ng/ml) for increasing times and subjected to immunoblot analysis with phospho-specific antibodies directed against p38 MAPK, ERK1/2, and JNK. First, using an antibody directed against MKP-1 we found that RANKL is a rapid and potent inducer of MKP-1 expression (Figure 6D). On RANKL stimulation of *mkp-1*$^{-/-}$ osteoclasts, the kinetics of ERK activation in the absence of MKP-1 was essentially equivalent to that of *mkp-1*$^{+/+}$ osteoclasts (Figure 6D). In contrast, p38 MAPK displayed an enhanced level of activation in response to RANKL in *mkp-1*$^{-/-}$ osteoclasts (Figure 6D). In addition, JNK exhibited both an enhanced and sustained activation in response to RANKL. These results suggest that MKP-1 negatively regulates osteoclast function by inactivation of MAPK-dependent signaling *in vitro*.

Osteoblasts Differentiated Independent of MKP-1

To investigate the potential contribution of osteoblasts to the bone phenotype of MKP-1-deficient mice, we set out to culture osteoblasts derived from marrow cells. Osteoblasts formed colonies, which generated calcified bone in the presence and in the absence of MKP-1, suggesting a discrete role, if any, for MKP-1 in osteoblasts (Figure 6E).

Discussion

In this study we demonstrate that MKP-1 plays a role in the control of adult bone mass via the differentiation and the activation of osteoclasts. We also report that RANKL is a potent inducer of MKP-1 expression, which subsequently attenuates MAPK activation in osteoclasts. The net level of protein phosphorylation of signaling molecules is representative of the sum, at any given time, of the opposing activities of kinases and phosphatases, which ultimately dictate the biological response. By virtue of dephosphorylating p38 MAPK and JNK, two molecules that play key roles in the differentiation and the activation of osteoclasts, MKP-1 seems to negatively regulate osteoclast differentiation and activation. In addition, our findings support the critical role of p38 MAPK and/or JNK in osteoclast activation. Recent evidence suggests that MKP-5 also plays a role in osteoclast function. MKP-5 is a member of the MKP family of dual-specificity phosphatases that predominately dephosphorylate JNK. MKP-5 was induced in osteoclasts after stimulation by RANKL.[28] RANKL-induced activation of MKP-5 was proposed to limit JNK activation as a mechanism to protect osteoclasts from undergoing apoptosis. It is conceivable that the relatively mild nature of the bone loss phenotype observed in female *mkp-1*$^{-/-}$ mice could be a result of other MKPs, such as MKP-5, embracing the role for MKP-1 in MKP-1-deficient mice. Indeed, the transient nature of the lower bone mass phenotype observed in female MKP-1-deficient mice could result from compensation by alternative MKPs. Nevertheless, our results are generally consistent with MKP-1 playing a major role in negatively regulating osteoclast activity. In addition to MKP-1 and MKP-5, the ERK-specific MKP, MKP-3, mediates the development of bone by signaling downstream of the fibroblast growth factor receptor.[29] Yet, in a ge-

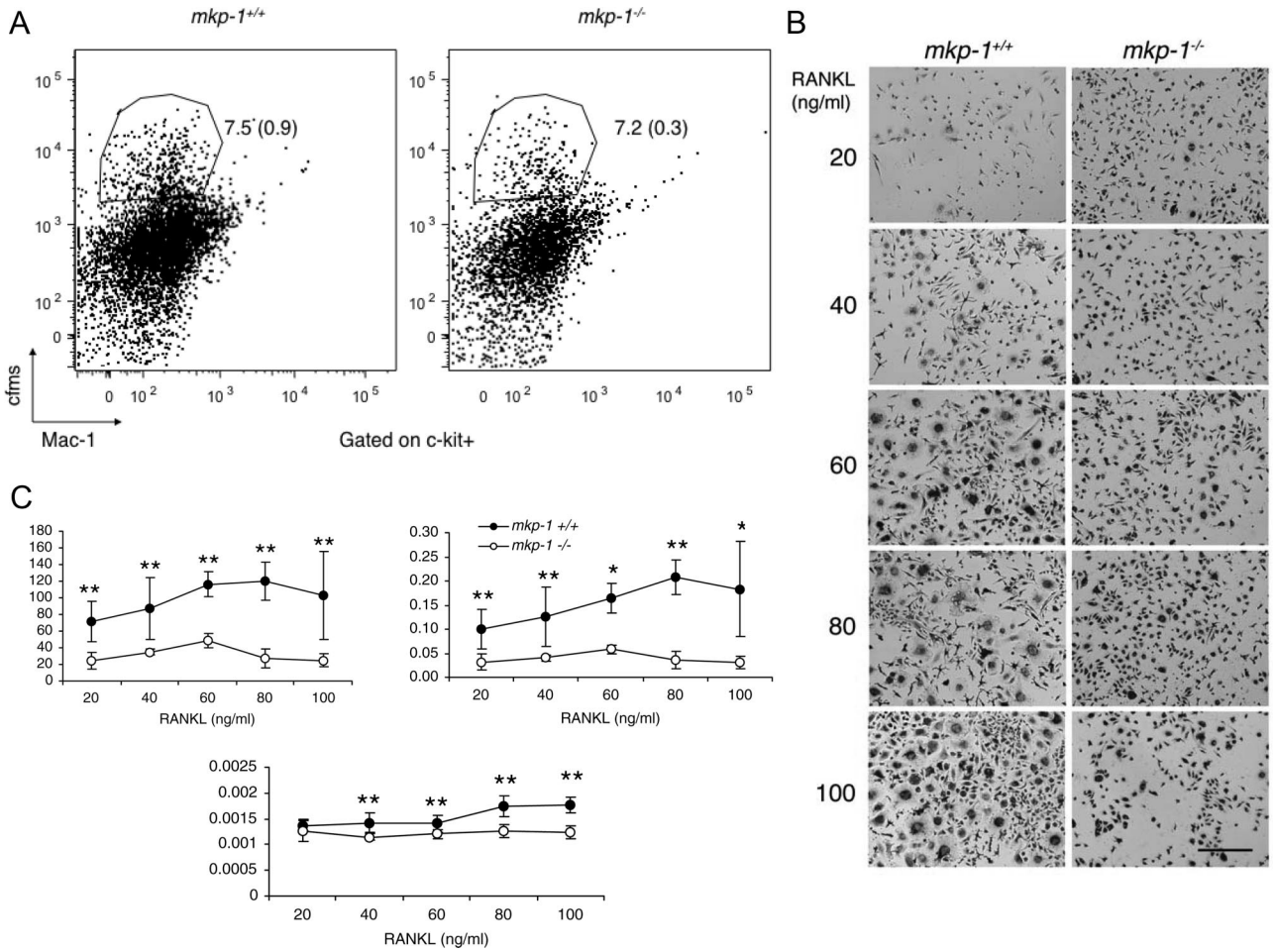

Figure 5. Absence of MKP-1 reduces osteoclastogenesis in response to M-CSF and RANKL. **A:** Bone marrow-derived macrophages from 6-week-old MKP-1-deficient and wild-type mice were cultured in the presence of M-CSF (30 ng/ml) for 2 days before being subjected to flow cytometric analysis with antibodies directed against c-fms, Mac-1, and C-kit, as surface markers. Note that the absence of MKP-1 did not affect the number of osteoclast precursor cells. $n = 3$. **B:** Spleen-derived macrophages were cultured for 6 days in the presence of M-CSF (20 ng/ml) and increasing concentrations of RANKL. Scale bar = 100 μm. Cells were stained for the osteoclast marker tartrate-resistant acid phosphates to record their number per well, the surface they occupy, with calculation of average cell size (**C**). $n = 5$. Data are means ± SD. $^{*}P < 0.05$ and $^{**}P < 0.01$.

nome-wide cDNA microarray analysis of fusing macrophages, we found that only MKP-1 is induced (data not shown). Therefore, despite their overlapping substrate specificities for the MAPKs, these observations collectively suggest an important role for each of the MKPs in bone development and homeostasis.

Given that MKP-1 functions as a stress-responsive gene we had anticipated that estrogen depletion-induced bone loss would be exacerbated in MKP-1-deficient mice. However, we observed that MKP-1-deficient mice exhibited similar levels of bone loss compared with wild-type mice after estrogen depletion. Yet, MKP-1-deficient mice had fewer osteoclasts. Because this experiment included control rather than sham-operated animals, it is possible that cortisol released in response to the stress induced by surgery prevented a stronger osteoclast response in MKP1-deficient mice.[30] These results suggested, however, that MKP-1-deficient mice had osteoclasts that were hyperactive and hence were capable of resorbing equal quantities of bone compared with wild-type mice. We confirmed these results by inducing rapid formation and activation of osteoclasts in calvariae. We also confirmed these results in cultured osteoclasts derived from MKP-1-deficient mice. Hence, it seems that MKP-1 regulation of the MAPKs not only controls osteoclast activity but also seems to play an important role in promoting the expansion of the osteoclast population itself. The question as to why only female mice show a discrete bone phenotype, which dissipates with age, remains open. We, and others, have reported similar gender differences in knockout mice.[24]

Although the MAPK pathway has been shown to stimulate both osteoclast and osteoblast differentiation, the lower bone mass phenotype observed in MKP-1-deficient young female mice was indicative of a predominant dysregulation in osteoclasts rather than in osteoblasts. Typically, the more osteoclasts, the more osteoblasts there are, accompanied by an increase in the turnover of bone. Here, perhaps because of the hyperactivated state of osteoclasts, osteoblast activity does not seem to be sufficiently enhanced *in vivo* because the rate of bone formation remains similar to that of wild-type mice in response to estrogen depletion. This observation suggested that perhaps the number

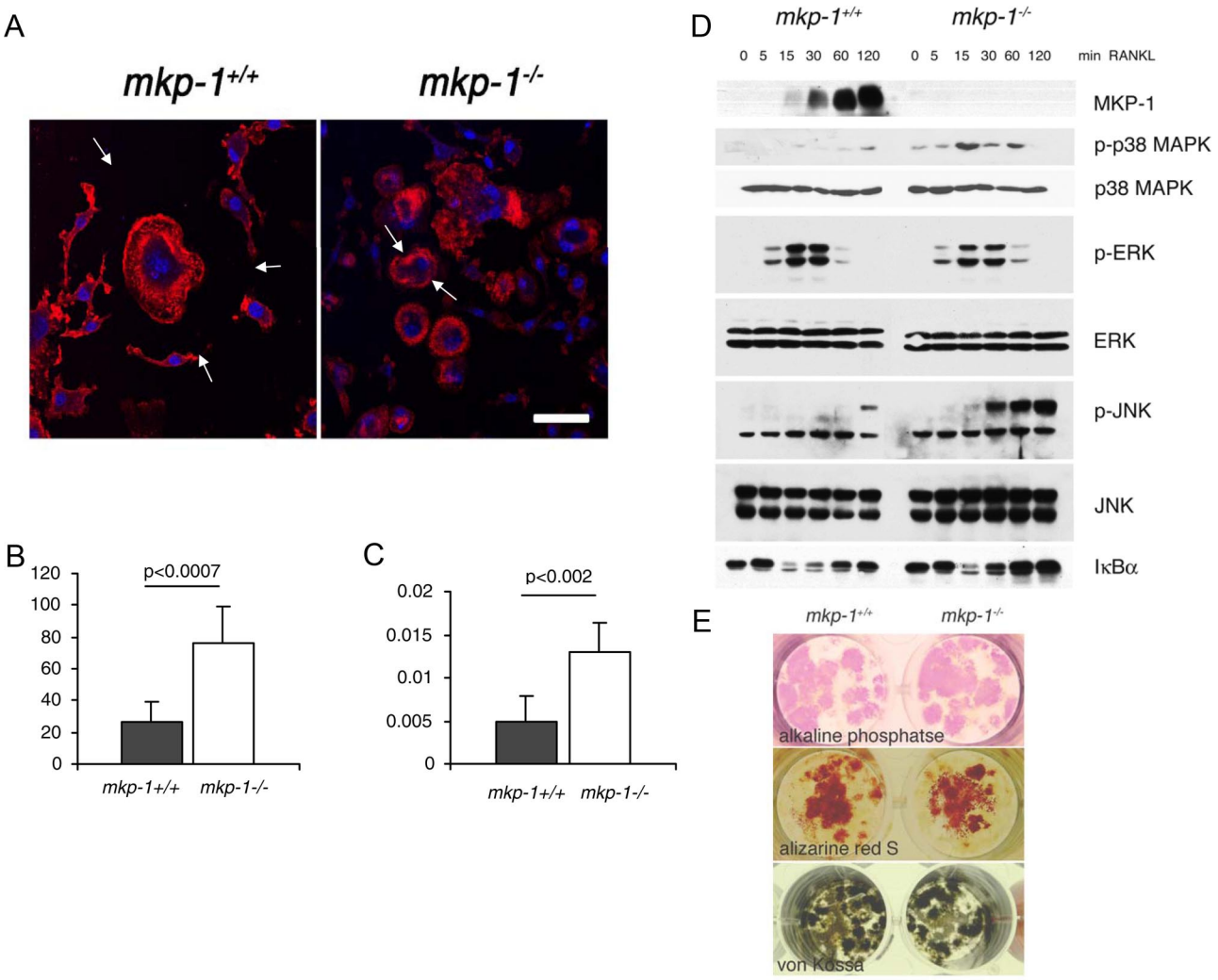

Figure 6. Enhanced osteoclast but not osteoblast activity in MKP-1-deficient mice. **A:** Spleen-derived macrophages were cultured in the presence of M-CSF (20 ng/ml) and RANKL (100 ng/ml) for 8 days and then were fixed and reacted with phalloidin-Alexa Fluor 568 and Topro-3. **Arrows** point out the extent of osteoclast plasma membrane. Scale bar = 20 μm. **B** and **C:** Spleen-derived macrophages were cultured in the presence of M-CSF (20 ng/ml) and RANKL (100 ng/ml) for 20 days on a calcium phosphate substrate. Osteoclast activity was assessed by recording the calcium phosphate surface area dissolved (**B**) and the number of resorbed areas (**C**) per well. Results are representative of three independent experiments. Data are means ± SD; $n = 3$. **D:** Bone marrow-derived macrophages isolated from *mkp-1*$^{+/+}$ and *mkp-1*$^{-/-}$ mice were cultured for 7 days in the presence of M-CSF (20 ng/ml) and RANKL (100 ng/ml). Cells were then serum-starved for 2 hours and activated with 100 ng/ml RANKL for the indicated times. Cell lysates were resolved and subjected to Western blotting with the indicated antibodies. Blots are representative of four separate experiments with similar results (see Table 3 for quantification). **E:** Bone marrow derived pre-osteoblasts were cultured for 7 days and then reacted for alkaline phosphate or cultured for an additional 7 days in the presence of β-glycerophosphate and stained with Alizarine red S or von Kossa stain.

rather than the activity of individual osteoclasts dictates the bone formation response.

Although p38 MAPK is currently being considered as a potential therapeutic target for inflammation-mediated bone loss (reviewed in Ref. [31]), our data suggest that activating MKP-1 rather than inhibiting p38 MAPK might offer a novel therapeutic avenue to control bone mass, whether general or local.

Table 3. Quantification of the Western Blot Data Illustrated in Figure 6D

	mkp-1+/+						*mkp-1*$^{-/-}$					
	0 min	5 min	15 min	30 min	60 min	120 min	0 min	5 min	15 min	30 min	60 min	120 min
MKP1	0 (0)	0 (0)	1232 (79)	1581 (129)	2123 (129)	2644 (139)	0 (0)	0 (0)	0 (0)	0 (0)	0 (0)	0 (0)
P-p38	0 (0)	0 (0)	0 (0)	0 (0)	213 (26)	162 (25)	181 (26)	168 (28)	567 (68)	567 (56)	279 (66)	0 (0)
P-ERK	0 (0)	207 (34)	638 (27)	638 (61)	156 (15)	0 (0)	176 (33)	502 (55)	518 (47)	186 (25)	0 (0)	0 (0)
P-JNK	0 (0)	0 (0)	0 (0)	0 (0)	0 (0)	252 (38)	0 (0)	0 (0)	100 (13)	796 (88)	906 (88)	1370 (145)
IκBα	584 (55)	820 (90)	376 (56)	376 (29)	601 (29)	701 (5)	974 (111)	891 (89)	496 (61)	584 (63)	864 (79)	864 (91)

Numbers represent arbitrary units (SD). $n = 4$.
IκBα, inhibitor of nuclear factor-κB.

Acknowledgments

We are grateful to Nancy Troiano and Chris Codi who helped process the bones and to Joshua VanHouten for his help with micro-CT analysis.

References

1. Cuevas BD, Abell AN, Johnson GL: Role of mitogen-activated protein kinase kinase kinases in signal integration. Oncogene 2007, 26:3159–3171
2. Keyse SM: Dual-specificity MAP kinase phosphatases (MKPs) and cancer. Cancer Metastasis Rev 2008, 27:253–261
3. Dickinson RJ, Keyse SM: Diverse physiological functions for dual-specificity MAP kinase phosphatases. J Cell Sci 2006, 119:4607–4615
4. Schindeler A, Little DG: Ras-MAPK signaling in osteogenic differentiation: friend or foe? J Bone Miner Res 2006, 21:1331–1338
5. Ducy P, Schinke T, Karsenty G: The osteoblast: a sophisticated fibroblast under central surveillance. Science 2000, 289:1501–1504
6. Blair HC, Zaidi M, Schlesinger PH: Mechanisms balancing skeletal matrix synthesis and degradation. Biochem J 2002, 364:329–341
7. Ge C, Xiao G, Jiang D, Franceschi RT: Critical role of the extracellular signal-regulated kinase-MAPK pathway in osteoblast differentiation and skeletal development. J Cell Biol 2007, 176:709–718
8. Yasuda H, Shima N, Nakagawa N, Yamaguchi K, Kinosaki M, Mochizuki S, Tomoyasu A, Yano K, Goto M, Murakami A, Tsuda E, Morinaga T, Higashio K, Udagawa N, Takahashi N, Suda T: Osteoclast differentiation factor is a ligand for osteoprotegerin/osteoclastogenesis-inhibitory factor and is identical to TRANCE/RANKL. Proc Natl Acad Sci USA 1998, 95:3597–3602
9. Lacey DL, Timms E, Tan HL, Kelley MJ, Dunstan CR, Burgess T, Elliott R, Colombero A, Elliott G, Scully S, Hsu H, Sullivan J, Hawkins N, Davy E, Capparelli C, Eli A, Qian YX, Kaufman S, Sarosi I, Shalhoub V, Senaldi G, Guo J, Delaney J, Boyle WJ: Osteoprotegerin ligand is a cytokine that regulates osteoclast differentiation and activation. Cell 1998, 93:165–176
10. Li J, Sarosi I, Yan XQ, Morony S, Capparelli C, Tan HL, McCabe S, Elliott R, Scully S, Van G, Kaufman S, Juan SC, Sun Y, Tarpley J, Martin L, Christensen K, McCabe J, Kostenuik P, Hsu H, Fletcher F, Dunstan CR, Lacey DL, Boyle WJ: RANK is the intrinsic hematopoietic cell surface receptor that controls osteoclastogenesis and regulation of bone mass and calcium metabolism. Proc Natl Acad Sci USA 2000, 97:1566–1571
11. Feng X: RANKing intracellular signaling in osteoclasts. IUBMB Life 2005, 57:389–395
12. Matsumoto M, Sudo T, Saito T, Osada H, Tsujimoto M: Involvement of p38 mitogen-activated protein kinase signaling pathway in osteoclastogenesis mediated by receptor activator of NF-κB ligand (RANKL). J Biol Chem 2000, 275:31155–31161
13. Lee ZH, Kim HH: Signal transduction by receptor activator of nuclear factor κB in osteoclasts. Biochem Biophys Res Commun 2003, 305:211–214
14. Huang H, Chang EJ, Ryu J, Lee ZH, Lee Y, Kim HH: Induction of c-Fos and NFATc1 during RANKL-stimulated osteoclast differentiation is mediated by the p38 signaling pathway. Biochem Biophys Res Commun 2006, 351:99–105
15. Shevde NK, Bendixen AC, Dienger KM, Pike JW: Estrogens suppress RANK ligand-induced osteoclast differentiation via a stromal cell independent mechanism involving c-Jun repression. Proc Natl Acad Sci USA 2000, 97:7829–7834
16. Srivastava S, Toraldo G, Weitzmann MN, Cenci S, Ross FP, Pacifici R: Estrogen decreases osteoclast formation by down-regulating receptor activator of NF-κB ligand (RANKL)-induced JNK activation. J Biol Chem 2001, 276:8836–8840
17. Chi H, Barry SP, Roth RJ, Wu JJ, Jones EA, Bennett AM, Flavell RA: Dynamic regulation of pro- and anti-inflammatory cytokines by MAPK phosphatase 1 (MKP-1) in innate immune responses. Proc Natl Acad Sci USA 2006, 103:2274–2279
18. Zhao Q, Wang X, Nelin LD, Yao Y, Matta R, Manson ME, Baliga RS, Meng X, Smith CV, Bauer JA, Chang CH, Liu Y: MAP kinase phosphatase 1 controls innate immune responses and suppresses endotoxic shock. J Exp Med 2006, 203:131–140
19. Salojin KV, Owusu IB, Millerchip KA, Potter M, Platt KA, Oravecz T: Essential role of MAPK phosphatase-1 in the negative control of innate immune responses. J Immunol 2006, 176:1899–1907
20. Hammer M, Mages J, Dietrich H, Servatius A, Howells N, Cato AC, Lang R: Dual specificity phosphatase 1 (DUSP1) regulates a subset of LPS-induced genes and protects mice from lethal endotoxin shock. J Exp Med 2006, 203:15–20
21. Maier JV, Brema S, Tuckermann J, Herzer U, Klein M, Stassen M, Moorthy A, Cato AC: Dual specificity phosphatase 1 knockout mice show enhanced susceptibility to anaphylaxis but are sensitive to glucocorticoids. Mol Endocrinol 2007, 21:2663–2671
22. Dorfman K, Carrasco D, Gruda M, Ryan C, Lira SA, Bravo R: Disruption of the erp/mkp-1 gene does not affect mouse development: normal MAP kinase activity in ERP/MKP-1-deficient fibroblasts. Oncogene 1996, 13:925–931
23. Wu JJ, Bennett AM: Essential role for mitogen-activated protein (MAP) kinase phosphatase-1 in stress-responsive MAP kinase and cell survival signaling. J Biol Chem 2005, 280:16461–16466
24. Li H, Cuartas E, Cui W, Choi Y, Crawford TD, Ke HZ, Kobayashi KS, Flavell RA, Vignery A: IL-1 receptor-associated kinase M is a central regulator of osteoclast differentiation and activation. J Exp Med 2005, 201:1169–1177
25. Cui W, Cuartas E, Ke J, Zhang Q, Einarsson HB, Sedgwick JD, Li J, Vignery A: CD200 and its receptor, CD200R, modulate bone mass via the differentiation of osteoclasts. Proc Natl Acad Sci USA 2007, 104:14436–14441
26. Ballica R, Valentijn K, Khachatryan A, Guerder S, Kapadia S, Gundberg C, Gilligan J, Flavell RA, Vignery A: Targeted expression of calcitonin gene-related peptide to osteoblasts increases bone density in mice. J Bone Miner Res 1999, 14:1067–1074
27. Bruzzaniti A, Baron R: Molecular regulation of osteoclast activity. Rev Endocr Metab Disord 2006, 7:123–139
28. Vaira S, Alhawagri M, Anwisye I, Kitaura H, Faccio R, Novack DV: RelA/p65 promotes osteoclast differentiation by blocking a RANKL-induced apoptotic JNK pathway in mice. J Clin Invest 2008, 118:2088–2097
29. Li C, Scott DA, Hatch E, Tian X, Mansour SL: Dusp6 (Mkp3) is a negative feedback regulator of FGF-stimulated ERK signaling during mouse development. Development 2007, 134:167–176
30. Rickard A, Young M: Corticosteroid receptors, macrophages and cardiovascular disease. J Mol Endocrinol 2009, 42:449–459
31. Wei S, Siegal GP: p38 MAPK as a potential therapeutic target for inflammatory osteolysis. Adv Anat Pathol 2007, 14:42–45